Bioscience, Biotechnology, and Biochemistry

ISSN: 0916-8451 (Print) 1347-6947 (Online) Journal homepage: http://www.tandfonline.com/loi/tbbb20

Quercetin inhibits advanced glycation end product formation via chelating metal ions, trapping methylglyoxal, and trapping reactive oxygen species

Mohammad Nazrul Islam Bhuiyan, Shinya Mitsuhashi, Kengo Sigetomi & Makoto Ubukata

To cite this article: Mohammad Nazrul Islam Bhuiyan, Shinya Mitsuhashi, Kengo Sigetomi & Makoto Ubukata (2017): Quercetin inhibits advanced glycation end product formation via chelating metal ions, trapping methylglyoxal, and trapping reactive oxygen species, Bioscience, Biotechnology, and Biochemistry, DOI: 10.1080/09168451.2017.1282805

To link to this article: http://dx.doi.org/10.1080/09168451.2017.1282805

Published online: 08 Feb 2017.

Bioscience, Biotechnology, and Biochemistry, 2017

Quercetin inhibits advanced glycation end product formation via chelating metal ions, trapping methylglyoxal, and trapping reactive oxygen species

Mohammad Nazrul Islam Bhuiyan[†], Shinya Mitsuhashi[†], Kengo Sigetomi and Makoto Ubukata*

Division of Applied Bioscience, Graduate School of Agriculture, Hokkaido University, Sapporo, Japan

Received September 27, 2016; accepted December 29, 2016
http://dx.doi.org/10.1080/09168451.2017.1282805

Physiological concentration of Mg^{2+}, Cu^{2+}, and Zn^{2+} accelerated AGE formation only in glucose-mediated conditions, which was effectively inhibited by chelating ligands. Only quercetin (10) inhibited MGO-mediated AGE formation as well as glucose- and ribose-mediated AGE formation among 10 polyphenols (1–10) tested. We performed an additional structure-activity relationship (SAR) study on flavanols (10, 11, 12, 13, and 14). Morin (12) and kaempherol (14) showed inhibitory activity against MGO-mediated AGE formation, whereas rutin (11) and fisetin (13) did not. These observations indicate that 3,5,7,4′-tetrahydroxy and 4-keto groups of 10 are important to yield newly revised mono-MGO adducts (16 and 17) and di-MGO adduct (18) having cyclic hemiacetals, while 3′-hydroxy group is not essential. We propose here a comprehensive inhibitory mechanism of 10 against AGE formation including chelation effect, trapping of MGO, and trapping of reactive oxygen species (ROS), which leads to oxidative degradation of 18 to 3,4-dihydroxybenzoic acid (15) and other fragments.

Key words: advanced glycation end products (AGEs); chelation effect; trapping ROS (reactive oxygen species); trapping MGO (methylglyoxal); hemiacetal form of di-MGO adduct

Polyphenols are ubiquitous secondary plant metabolites, and their most important dietary sources are fruits, vegetables, soybeans and beverages including green and black tea, red wine, and beer. These ingredients gather plenty of attention because they have many potential effects for human health to treat diabetes, allergy, asthma, cancer, cardiovascular disease, inflammation, and viral infectious disease.[1)] Especially, the effectiveness of flavonoids for inhibition of advanced glycation end product (AGE) formation has aroused many researchers' interest.[2–11)] Although the restrictive mechanism, that flavonoids can scavenge such reactive carbonyl species as methylglyoxal (MGO) and glyoxal (GO), has been proposed,[3,5–7,10,12–14)] as far as we know, the comprehensive action mechanism of flavonoids against AGE formation has not been fully elucidated. In this article, we describe how quercetin, one of the most abundant flavonols, efficiently inhibits the formation of advanced glycation end products (AGEs).

To determine the impact of metal ions on AGE formation, we first performed the assays with or without physiological concentration of Mg^{2+}, Cu^{2+}, and Zn^{2+} in glucose-, ribose-, and MGO-mediated AGE formations. The structure-activity relationships of polyphenols were determined using total 10 polyphenols: two catechin monomers, (−)-epicatechin (**1**) and (−)-epigallocatechin (**2**); a natural derivative of catechin, (−)-epigallocatechin-3-gallate (**3**); gallic acid (**4**), which is found both as free acid and as part of hydrolysable tannin; a catechin dimer, procyanidin B2 (**5**); a catechin trimer, procyanidin C1 (**6**); two isoflavons, genistein (**7**) and daizein (**8**); a flavanone, hesperetin (**9**); and a flavonol, quercetin (**10**). Quercetin (**10**) showed most potent inhibitory effects in glucose-mediated or ribose-mediated AGE formation assay, then we found a positive correlation between the presence of chelating site and inhibitory effects against glucose-mediated AGE formation. Only quercetin (**10**) inhibited MGO-mediated AGE formation, we therefore investigated the structure requirement for inhibitory effect of flavonol comparing **10** with rutin (**11**), morin (**12**), fisetin (**13**), and kaempferol (**14**). Ketone at C-4 and 3,5,4′-triol of quercetin (**10**) seem to be essential for inhibition of MGO-mediated AGE formation. Li et al. proposed the trapping mechanism in which aldehyde moieties of one or two equivalents of MGO were directly attacked by C-6 and C-8 of **10** to form quercetin mono-MGO adduct and quercetin di-MGO adduct base on LC-MS/MS analysis.[10)] We suspected their proposed structures of MGO adducts and isolated sufficient amounts of these compounds by inhibiting degradation under oxygen-free conditions. The true structures of MGO adducts were finally determined to be cyclic hemiacetals (**16**, **17** and **18**) by NMR analysis including NMR chemical shift calculations for each possible structure. We propose a new

*Corresponding author. Email: m-ub@for.agr.hokudai.ac.jp
[†]These authors contribute equally in this work.

inhibitory mechanism of **10** against MGO-mediated AGE formations.

Materials and methods

Chemicals and reagents. 3,4-Dihydroxybenzoic acid and argon gas were purchased from Tokyo Chemical Industry (Tokyo, Japan) and Air Water Inc. (Osaka, Japan), respectively. Methylglyoxal (MGO) solution (~40% in H_2O), bovine serum albumin (BSA), dimethyl sulfoxide (DMSO), diethylenetriaminepentaacetic acid (DTPA), phosphate buffer saline (PBS, pH 7.4), MeOH-d_4, DMSO-d_6, $CuSO_4$, $ZnSO_4$, $MgSO_4$, and 96-well clear bottom plates were purchased from Sigma-Aldrich (St. Louis, MO, USA). HPLC grade solvents were from Kanto Chemical Co. Inc. (Tokyo, Japan), quercetin dihydrate and other reagents were from Wako Co. (Osaka, Japan). All chemicals were of analytical grade.

Glucose-, ribose-, and methylglyoxal (MGO)-mediated AGE formation assay. BSA-glucose glycation and fluorescence detection of protein adducts were performed *in vitro* as previously described method[2] with slight modifications. BSA-ribose or BSA-MGO assay were conducted by essentially the same method except for using ribose or MGO instead of glucose. In brief, 500 μL of reaction mixture containing 0.8 mg/mL BSA, 200 mM ribose or 5 mM MGO with or without 2.5 μL of 20 mM compound in 50 mM phosphate buffer (pH 7.4) was prepared, and the reaction was allowed to proceed at 37 °C for 24 h for BSA-ribose or 16 h for BSA-MGO assay. Trace metals, $CuSO_4$ (0.75 μM), $ZnSO_4$ (0.25 μM), and $MgSO_4$ (0.7 mM) were added in each reaction mixture to evaluate the impact of metal ions on AGE formation. DTPA (0.1 mM and 1 mM) and 100 mM of aminoguanidine (AG, 1 mM) were used for positive controls as chelating agent and glycation inhibitor, respectively. The fluorescence intensity (ex. 360 nm, em. 465 nm) of AGE-related protein was measured using GENios FL Fluorescent Microplate Reader (Tecan, Mannedorf, Switzerland). The inhibitory activity was calculated by subtracting the quenching effect for the apparent inhibitory activity. One way-analysis of variance (ANOVA), Tukey-Kramer method, and paired *t*-test were implemented to determine statistical significance in a software package, KaleidaGraph, ver 4.1 (Synergy Software, Reading, PA, USA).

*Large-scale preparation of reaction products derived from quercetin (**10**) in MGO-mediated AGE formation assay.* Quercetin (**10**) (34 mg) was dissolved in 1 liter reaction solution consisting of 50 mM phosphate buffer (pH 7.4) containing 0.8 mg/mL BSA, 0.7 mM $MgSO_4$, 0.75 μM $CuSO_4$, and 0.25 μM $ZnSO_4$. To the resultant solution, 770 μL of H_2O (control mixture) or 770 μL of 40% MGO (MGO mixture) was added. The ratio of **10** to MGO was 1:50 in which conditions were the most effective to obtain sufficient amounts of the reaction products in our experiment. The control mixture was immediately frozen and stored at –83 °C until use as an analytical control. The MGO mixture was incubated at 37 °C for 16 h. The resultant mixture was freeze-dried for 36 h, then allowed to melt for 12 h, and finally freeze-dried again for another 5 days. The freeze-dried sample was extracted four times with MeOH, and the combined solution was filtrated with 0.2 μm filter. The filtrate was concentrated *in vacuo*, dissolved in DMSO, and purified by preparative ODS C18 column (20 × 250 mm, 5 μm, Mightysil) using a Hitachi HPLC system equipped with a diode array detector. Millipore water with 0.1% AcOH and HPLC grade MeOH with 0.1% AcOH were used for elution as mobile phase B and mobile phase A, respectively. Flow rate was 5 mL/min, and the isocratic HPLC conditions were as follows: 0–30 min, 10% A and 90% B followed by 15 min re-equilibration of the column with UV detection at 254 nm. The injection volume was 200 μL, and 4.2 mg of **15**, 0.2 mg of **16**, 0.5 mg of **17**, and 1.2 mg of **18** were isolated, and each sample was stored at –20 °C until use for nuclear magnetic resonance (NMR) and electrospray ionization mass spectrometry (ESI-MS) analyses.

*Quantitative analysis of the products derived from **10** in MGO-mediated AGE formation.* Quercetin (**10**) (10.2 mg) was dissolved in 300 mL reaction solution consisting of 50 mM phosphate buffer (pH 7.4) containing 0.8 mg/mL BSA, 0.7 mM $MgSO_4$, 0.75 μM $CuSO_4$, 0.25 μM $ZnSO_4$. The resultant solution (300 mL) was divided into three equal parts (100 mL each). Seventy-seven μL of H_2O was added instead of MGO solution to the first sample (100 mL), and the control reaction was referred to as Condition **A**. This sample was immediately frozen at –83 °C. Second sample (100 mL) was used for the conventional experiment with 77 μL of 40% MGO and the reaction was referred to as Condition **B**. The ratio of **10** to MGO was 1:50. This sample was also immediately frozen at –83 °C. Third sample (100 mL) was used for the experiment with 77 μL of 40% MGO (10 mM) under oxygen-free conditions and the reaction was referred to as Condition **C**. The ratio of **10** to MGO was 1:50. Removal of oxygen from the reaction mixture was conducted by gas change with argon using freeze-pump-thaw technique. This sample was immediately frozen and stored at –83 °C until use. Each sample was incubated at 37 °C for 16 h, kept in a freezer at –83 °C for 40 min to quench the reaction, and then lyophilized. The freeze-dried sample was extracted four times with MeOH, and the combined solution was filtrated with 0.2 μm filter. The filtrate was concentrated *in vacuo*, and stored in freezer at –20 °C until analysis. HPLC analysis of each MeOH extract was performed on a Hitachi HPLC system equipped with a diode array detector. Oxidative product **15**, MGO-quercetin adducts **16**, **17**, **18**, and starting material **10** were quantified with UV detection at 254 nm using analytical ODS C18 column (4.6 × 250 mm, 5 μm, Mightysil). HPLC conditions were the same as those for preparative HPLC except for flow rate, 1 mL/min and injection volume, 20 μL.

NMR and ESI-MS analyses. NMR measurements including ^{1}H-^{1}H COSY, ^{13}C DEPT-135 (distortionless enhancement by polarization transfer), HSQC (heteronuclear single quantum correlation) and HMBC (heteronuclear multiple bond correlation) of **15** in MeOH-d_4, **16**, **17**, and **18** in DMSO-d_6 were performed with a Bruker AMX-500 (Bruker, MA, USA) at GC-MS & NMR Laboratory, Faculty of Agriculture, Hokkaido University. Chemical shift was reported in δ ppm using tetramethylsilane as the internal standard, and coupling constants (J) were given in hertz. All ESI-MS spectra were recorded on LTQ-Orbitrap XL (ThermoScientific, MA, USA) using a Paradigm MS2 (Michrom BioResources, CA, USA). NMR chemical shifts of **16**, **17**, **18**, and their isomers were predicted using ChemNMR (Upstream Solutions, Zurich, Switzerland) in ChemDraw Ultra, ver. 12.0 (CambridgeSoft, MA, USA).

Results and discussion

Impact of metal ions in AGE formation

Chelation is one of the fundamental mechanisms of action occurring in wide range of polyphenols[15,16] that may affect AGE formation in diabetes. AGE inhibitors may act primarily as chelators, because metal-catalyzed oxidation reactions accelerate AGE formation.[17]

In this study, the effects of physiological concentration of metal ions, Cu^{2+}, Zn^{2+}, and Mg^{2+} were investigated on glucose-, ribose-, and MGO-mediated AGE formation. Surprisingly, only glucose-mediated AGE formation was significantly enhanced by metal ions, whereas it was remarkably inhibited by DTPA having high affinity for metal cations ($p < 0.01$). These results suggested that metal ions were indispensable for the AGE formation mediated by glucose. Although ribose-mediated AGE formation was slightly enhanced by metal ions ($p < 0.05$), MGO-mediated AGE formation was not affected by these metal cations. Aminoguanidine (AG) exhibited inhibitory activity against glucose-, ribose-, and MGO-mediated AGE formation in the presence of metal ions as shown in Fig. 1. It is possible to explain why the effect of metal ions was far weaker in ribose-mediated AGE formation than in glucose-mediated AGE formation. A study revealed that ribose is an effective glycation agent compared to glucose both *in vitro* and *in vivo*.[18] Conformational change from helix to β-sheet occurs during glycation of lysozyme, and rapid perturbation of the tertiary structure occurs in the presence of ribose.[19] In addition, divalent metal ions bind to 2,3-vicinal diol of ribose in aqueous solution,[20,21] whereas glucose chelates such metal ions very poorly at neutral pH.[22] A potent chelating effect of ribose might be a factor for accelerating AGE formation by coordinating the ribose–metal complex to arginine, lysine, asparagine, glutamine, aspartic acid, or glutamic acid residue of protein.[23,24] Glucose, which has weak chelating effect needs additional amounts of metal ions for acceleration of AGE formation. Thus chelating effect of inhibitor may be a limiting factor for glucose-mediated AGE formation, whereas it would be only a minor factor for ribose-mediated AGE formation.

*Structure–activity relationships (SARs) on fourteen different polyphenols (**1–14**)*

To analyze structure–activity relationships (SARs) between inhibitory activity against AGE-formation and polyphenols, namely (–)-epicatechin (**1**), (–)-epigallocatechin (**2**), (–)-epigallocatechin gallate (**3**), gallic acid (**4**), procyanidin B2 (**5**), procyanidin C1 (**6**), genistein (**7**), daidzein (**8**), hesperetin (**9**), quercetin (**10**), and four other flavonols (**11–14**), we evaluated the effects of these polyphenols using three different types of assay systems (Fig. 2). Since the inhibitory effect of chelating agent was confirmed in glucose-mediated AGE formation as shown in Fig. 1, inhibitory effects on glucose-, ribose-, and MGO-mediated AGE formation were investigated using polyphenols having potent (**1**, **2**, **3**, **4**, **5**, **6**, **10**), weak (**7**, **9**), or no (**8**) chelating unit as shown in Fig. 2.

Such polyphenols having vicinal diol as **1**, **2**, **3**, **4**, **5**, **6**, and **10** exhibited the significant inhibitory activities on glucose- and ribose-mediated AGE formation, whereas such polyphenols having C-4 keto and C-5 hydroxy groups as genistein (**7**) and hesperetin (**9**) showed only moderate inhibitory activities in glucose-mediated AGE formation ($p < 0.01$). Daidzein (**8**) lacking the typical metal chelation site did not inhibit AGE formation mediated by glucose (Fig. 2(a)).

These results suggested that chelating effects of polyphenols were important for their inhibitory activity on AGE formation, especially on glucose-mediated AGE formation. Meanwhile, all these polyphenols including daidzein (**8**) showed inhibitory activities against ribose-mediated AGE formation ($p < 0.01$), while quercetin (**10**) exhibited most potent inhibitory activities against both glucose- and ribose-mediated AGE formation (Fig. 2(a)). In addition, only **10** significantly inhibited MGO-mediated AGE formation among the above 10 polyphenols as indicated in Fig. 2(b).

Quercetin (**10**) was thus found to be the most potent inhibitor against glucose-, ribose-, and MGO-mediated AGE formations among the test compounds (**1–10**). The flavonol **10** was therefore considered as a standard AGE inhibitor in comparison with other flavonoids**.** To determine the structural requirements of quercetin (**10**) as the inhibitor of MGO-mediated AGE formation, such other flavonols as rutin (**11**), morin (**12**), fisetin (**13**), and kaempferol (**14**) were evaluated for their effects on MGO-mediated AGE formation as indicated in Fig. 2(b). The importance of C-3 hydroxy group and C-5 hydroxy group of **10** was confirmed using rutin (**11**) whose C-3 hydroxy was blocked by glycosylation and fisetin (**13**) lacking C-5 hydroxy group. Both **11** and **13** lost efficacies against MGO-mediated AGE formation.

Catechol moiety was considered to act as the essential functional group for metal chelation in epicatechin (**1**), epigallocatechin (**2**), epigallocatechin gallate (**3**), gallic acid (**4**), procyanidin B2 (**5**), procyanidin C1 (**6**), quercetin (**10**), rutin (**11**), or fisetin (**13**). These compounds inhibited glucose-mediated and ribose-mediated AGE formation, but compounds **1–6**, **11**, and **13** did not have efficient inhibitory activities against MGO-mediated AGE formation.

Thus, it seemed that the inhibitory effect of quercetin (**10**) against MGO-mediated AGE formation was

Table 1. ^{1}H and ^{13}C NMR data of isolated 3,4-dihydroxybenzoic acid (**15**) in MeOH-d_4.

Position	$^{\delta}C$, type	$^{\delta}H$, (*J* in Hz)	HMBC
C=O	171.2, s		
1	124.2, s		
2	118.6, d	7.43, d, 1H (2.1)	3, 4, 6, C=O
3	146.8, s		
4	152.2, s		
5	116.6, d	6 6.80, d, 1H (8.1)	3, 4, 1
6	124.7, d	7.41, dd, 1H (8.1, 2.1)	2, 4, C=O

regulated by other mechanisms. Since morin (**12**) and kaempferol (**14**) still retained their inhibitory activities against MGO-mediated AGE formation, C-3′ hydroxyl group seemed not to be essential for the inhibitory activity of **10** against MGO-mediated AGE-formation. Due to many evidences that increase in MGO levels in serum can lead to development of diabetic complications,[25–27] many scavenging agents such as aminoguanidine, tenilsetam, metformin, and pyridoxamine were introduced.[28,29] However, the side effects of these agents have prompted a search for less toxic MGO-trapping agents. Li et al. independently reported quercetin (**10**) as an efficient MGO-trapping agent.[10]

*Identification of 3,4-dihydroxybenzoic acid (**15**) derived from quercetin (**10**) in MGO-mediated AGE formation*

The structures of mono-MGO and di-MGO adducts of quercetin (**10**) in MGO-mediated AGE formation have been proposed based on LC-MS/MS analyses.[10] However, there are yet no rigorous evidence for the

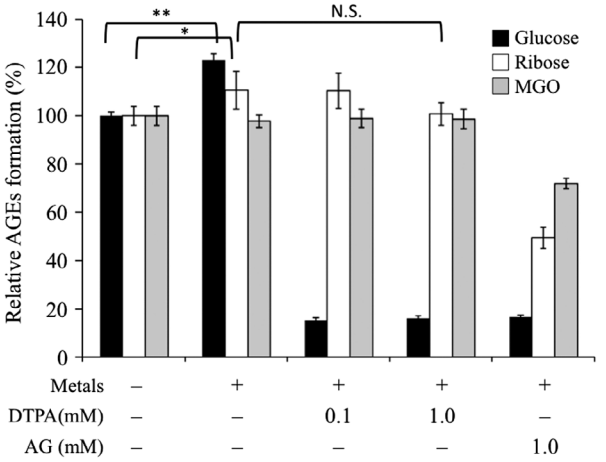

Fig. 1. Effects of metal ions in glucose-BSA, ribose-BSA, and MGO-BSA mediated AGE formation.

Notes: Diethylenetriaminepentaacetic acid (DTPA) and aminoguanidine (AG) were used as positive controls for removal of metal ions and for inhibition of AGE formation, respectively. Bars represent mean ± standard deviation of triplicate values. Paired *t*-test: $^{**}p < 0.01$, $^{*}p < 0.05$, N.S. p = not significant).

structures of MGO adducts of **10** or other flavonols. To determine the structures of MGO-quercetin adducts more precisely, we conducted the 1-L scale reaction of **10** with MGO in the presence of BSA and metal ions. Contrary to expectation, the major product in this reaction showed a pseudo-molecular ion at *m/z* 153 $[M\text{-}H]^{-}$ in the negative-ion ESI-MS. High-resolution electrospray ionization mass spectrometry (HR-ESI-MS) indicated the molecular formula of $C_7H_6O_4$ for the major compound. UV-visible spectrum showed

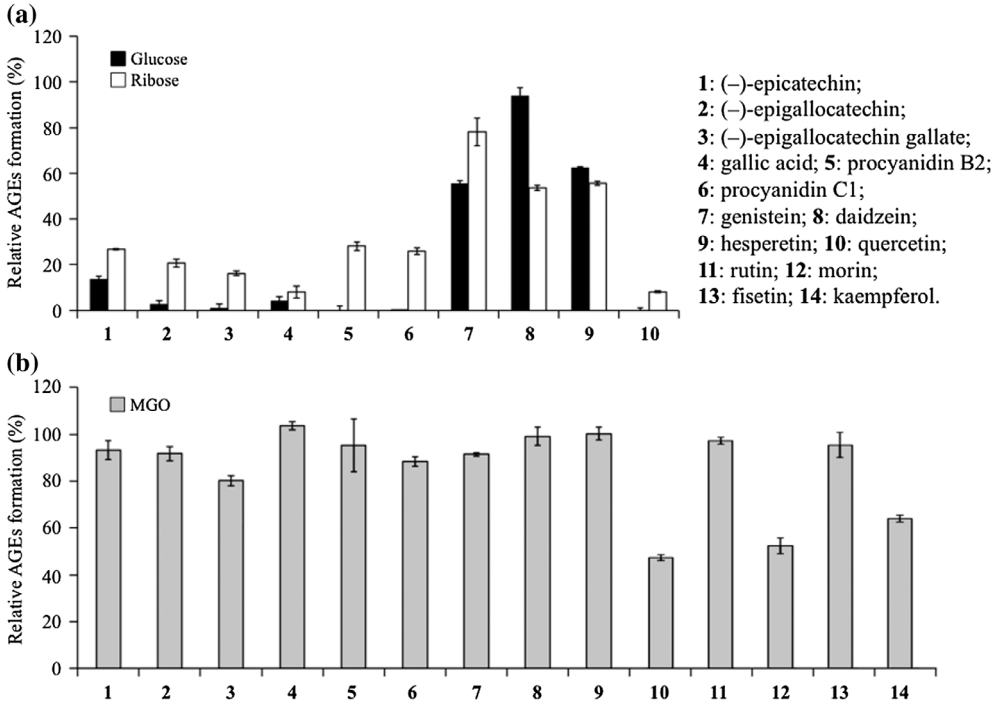

Fig. 2. Inhibitory effects of polyphenols against glucose-BSA, ribose-BSA, and MGO-BSA mediated AGE formation.

Notes: (a) Glucose- or ribose-mediated AGE formation in the presence of each polyphenol (**1–10**). (b) MGO-mediated AGE formation in the presence of each polyphenol (**1–14**). The concentration of each compound was 100 μM. Bars represent mean ± standard deviation of triplicate values.

three peaks at 210, 260, and 294 nm, respectively. The structure of the major product was unambiguously determined to be 3,4-dihydroxybenzoic acid (**15**) by ^{1}H NMR and ^{13}C NMR including 2D NMR analyses (Table 1), which was further confirmed by comparing it with an authentic sample by HPLC**.**

It was suggested that oxidative degradation of **10** proceeded to give **15** by prolonged treatment with dissolved oxygen in the reaction mixture. If this hypothesis was correct, the formation of **15** should be suppressed by removing oxygen from the reaction mixture in the assay system. To confirm this, we designed three different experiments including anoxic conditions.

*Productivities of 3,4-dihydroxybenzoic acid (**15**) and MGO-quercetin adducts (**16**, **17**, and **18**) from **10** in BSA-metal ion solution with or without MGO under ambient or anoxic conditions*

A model system under anoxic conditions provided a sufficient amount of MGO-quercetin adducts as expected (Fig. 3). The objective of the newly designed experiments was mainly to confirm the impact of oxygen. The first experiment was performed in a reaction mixture of quercetin (**10**) without MGO in the presence of BSA and metal ions. In this condition, the starting material **10** was detected as a single peak in HPLC shown as Condition **A** in Fig. 3(a) and (b). In second experiment, a 1:50 mixture of **10** and MGO was incubated in the presence of BSA and metal ions, and five remarkable products were detected in HPLC indicated as Condition **B** in Fig. 3(a) and (b). The products purified by HPLC were determined to be 3,4-dihydroxybenzoic acid (**15**), two mono-MGO adducts (**16** and **17**), di-MGO adduct (**18**), and the starting material **10** by ESI-MS spectral analyses. The third experiment was performed in a 1:50 reaction mixture of quercetin (**10**) and MGO in the presence of BSA and metal ions under anoxic conditions. In this reaction, the major product was assigned to be **18** and two minor products were assigned to be **16** and **17** by HPLC as shown in Condition **C** in Fig. 3(a) and (b). The structures were confirmed by HR-ESI-MS of isolated samples.

These results indicated that trapping of MGO in **10** proceeded without involvement of oxygen and resultant di-MGO adduct (**18**) was degraded by oxygen to give **15** under the ambient air level as indicated in Fig. 4.

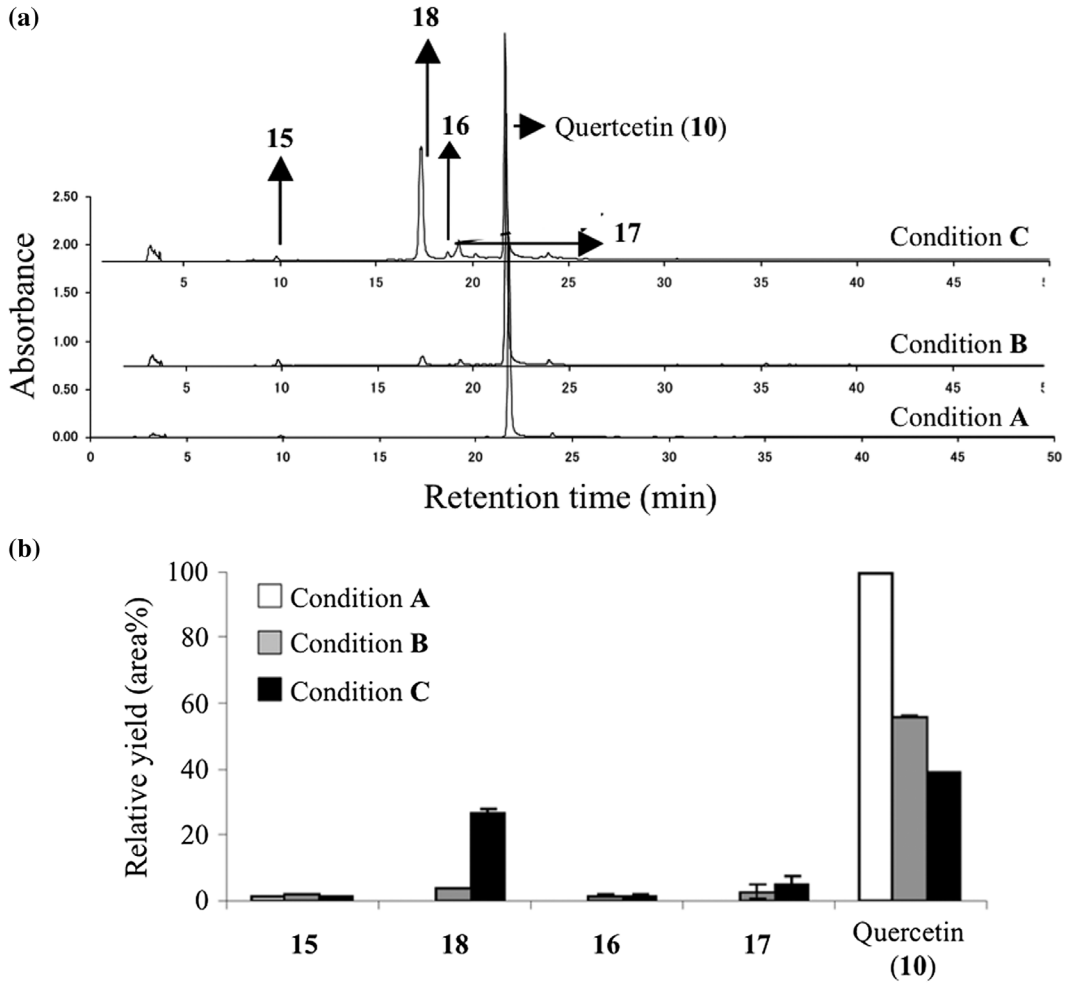

Fig. 3. Quantitative analysis of degradation product (**15**), MGO adducts (**16**, **17**, **18**) and quercetin (**10**).

Notes: (a) HPLC profiles of the samples originated from Condition **A** without MGO, Condition **B** with MGO, and Condition **C** with MGO under an argon atmosphere. Column conditions: Mightysil (4.6 × 250 mm, 5 μm), 10% mobile phase A (H_2O, 0.1% AcOH) and 90% mobile phase B (MeOH, 0.1% AcOH), 1.0 mL/min. Detection wavelength: 254 nm. (b) The relative yield of oxidative degradation product (**15**), di-MGO quercetin adduct (**18**), mono-MGO quercetin adducts (**16** and **17**), and reduction rate of quercetin (**10**) in MGO-mediated AGE formation under Condition **A**, Condition **B** or Condition **C**. The relative yield was calculated from each peak area value at 254 nm in HPLC.

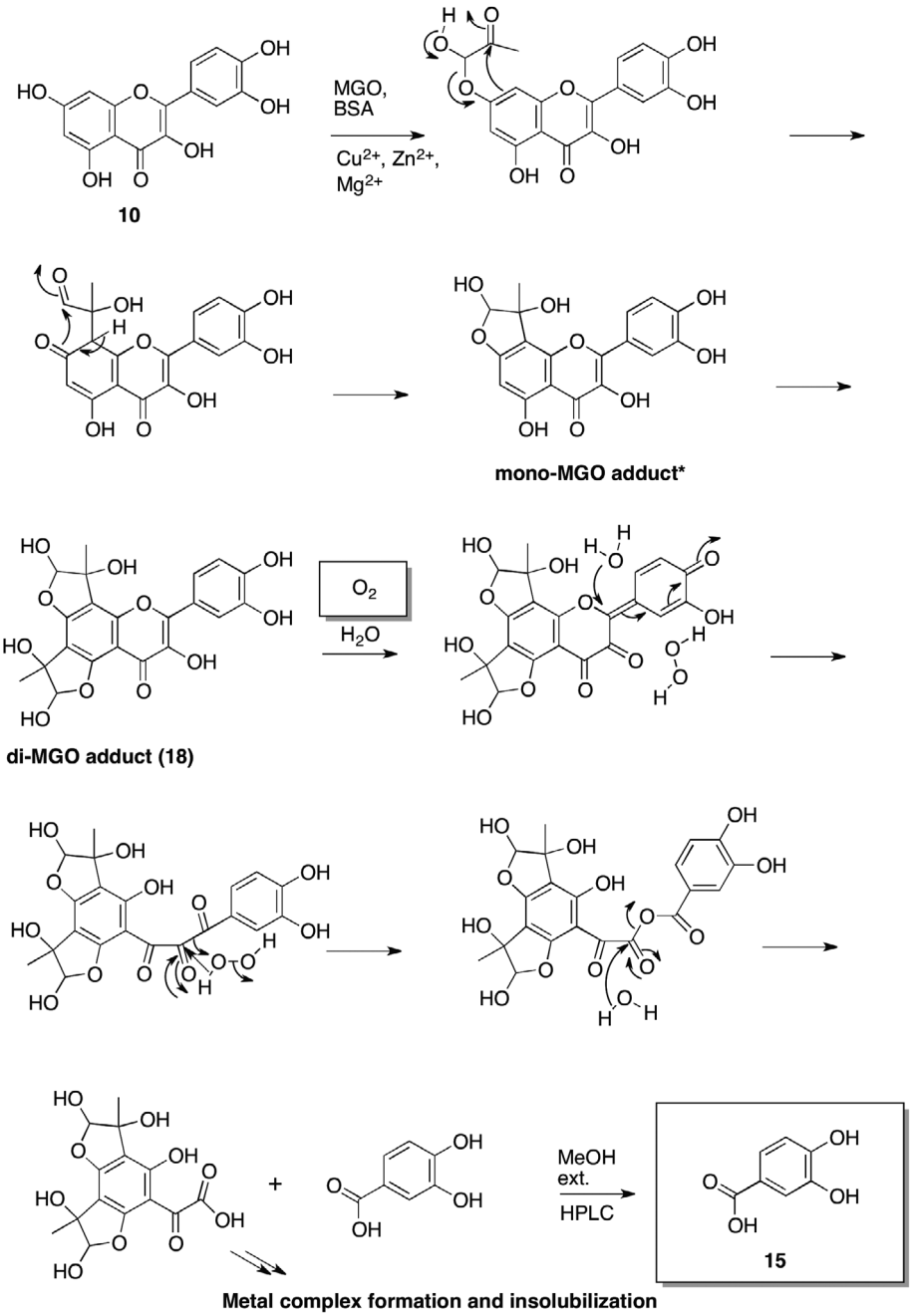

Fig. 4. Proposed mechanism for the fate of quercetin (10) in MGO-mediated AGE formation under ambient air conditions.
Notes: *Mono-MGO adduct (**17**) is shown as a representative. Trapping of two equivalent of MGO by quercetin (**10**) followed by trapping of one equivalent of reactive oxygen species at C2 position of di-MGO adduct (**18**) to give 3,4-dihydroxy benzoic acid (**15**).

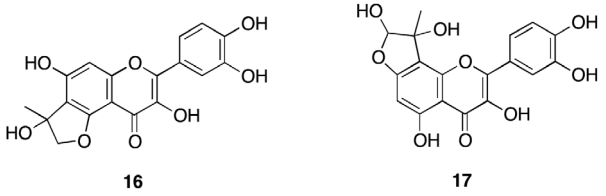

Fig. 5. Structure of mono-MGO adducts, 16 and 17.

*The structures of mono-MGO adducts (**16** and **17**) identified by HR-ESI-MS*

Mono-MGO adducts (**16** and **17**) indicated the same pseudo molecular ion at *m/z* 373 $[M\text{-}H]^-$ in negative ion mode. The molecular formulas of **16** and **17** were determined to be $C_{18}H_{14}O_9$ by HR-ESI-MS. Fig. 5 indicates the possible structures of **16** and **17** based on the molecular formula of each compound and NMR assignment of di-MGO adduct (**18**) shown in Fig. 6(a). The structure of mono-MGO adduct (**17**) was supported by its NMR using 0.5 mg of the sample and NMR chemical shift calculations for hemiacetal or hemiketal of mono-MGO adducts (Fig. 6(b)).

*Structural determination of di-MGO adduct (**18**) and fate of quercetin (**10**) in MGO-mediated AGE formation*

The structural information of di-MGO adduct (**18**) was obtained from NMR and ESI-MS in negative ion

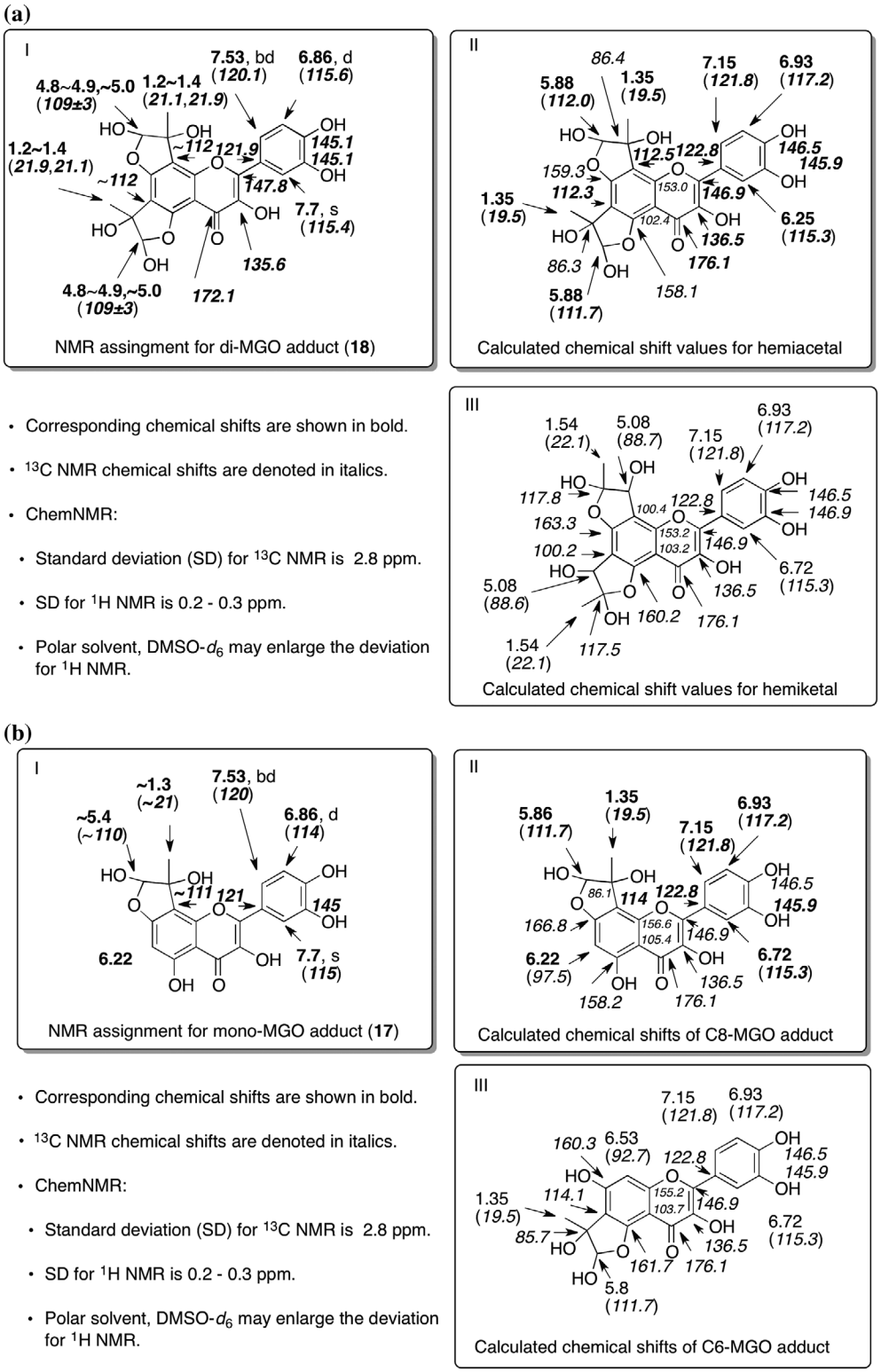

Fig. 6. Structure determination of di-MGO adduct (**18**) and mono-MGO (**17**).

Notes: (a) Observed NMR chemical shifts of **18** (I) and chemical shifts calculated for hemiacetal (II) or hemiketal (III). Hemiketal can be formed from di-MGO adduct of quercetin proposed by Li et al. [10] (b) Observed NMR chemical shifts of **17** (I) and chemical shifts calculated for two possible structures (II and III). ChemNMR was used for chemical shift calculations of ^{1H} and ^{13C} NMR in each structure on ChemDraw Ultra, ver. 12.0.3.1216 (CambridgeSoft Corp, Cambridge, MA, USA).

mode, indicating a pseudo molecular ion at *m*/*z* 445 $[M\text{-}H]^-$. Molecular formula of **18** was determined to be $C_{21}H_{18}O_{11}$ by HR-ESI-MS. Although limited amount of **18** existed as at least 8 distinguishable diastereomers made it difficult to assign completely the NMR signals, ^{1}H NMR supported the proposed structure of **18** indicating a singlet at 7.7 ppm for 2′-H and a pair of doublets at 7.5 and 6.86 ppm for 6′-H and 5′-H in B ring, respectively, whereas no proton signal at C-6 and C-8 in A ring was observed. HMQC of **18** indicated that 4 singlet protons at 4.8–4.9 ppm assigned as hemiacetal protons correlated with the carbon signals at

around 101 ppm, whereas C–H correlations for 4 singlet protons at around 5.0 ppm could not be detected due to the lack of adequate S/N ratio, while 8 singlet protons at 1.2–1.4 ppm assigned to methyl protons correlated with carbons at around 16 and 21.9 ppm. Meanwhile HMBC of **18** showed the long-range couplings between the methyl protons at 1.2–1.4 ppm and carbons approximately at 106–112 ppm assigned to C6, C8, and hemiacetal carbon.

Figure 6(a) indicates the comparison between NMR assignment of di-MGO adduct (**18**) and NMR chemical shifts calculated for newly proposed hemiacetal and for hemiketal which can be formed from di-MGO adduct proposed by Li et al.[10] The NMR data of **18** coincided with the NMR chemical shifts for hemiacetal rather than hemiketal. Aldehyde of MGO can be attacked first by phenolic oxygen atom, which makes possible to move the methyl ketone moiety closer to C6 or C8 in **10**. The optimal orientation effect could accelerate intramolecular aromatic substitution at C6 or C8 to form **18** as shown in Fig. 4. When quercetin (**10**) was incubated with MGO at a ratio of 1:50 in the presence of BSA and metal ions under anoxic conditions, the accumulation of di-MGO adduct (**18**) was remarkably enhanced in comparison with 3,4-dihydroxybenzoic acid (**15**) or mono-MGO adducts (**16** and **17**). The amount of unreacted quercetin (**10**) also dramatically decreased in this experiment as shown in condition **C** of Fig. 3. The structure of di-MGO adduct (**18**) and overall oxidative degradation steps are illustrated in Fig. 4.

Conclusion

Structure–activity relationship (SAR) studies on 10 polyphenols (**1–10**) indicated that quercetin (**10**) was the most potent inhibitor against AGE formation in glucose-, ribose-, or MGO-mediated assay system. The structural requirements of **10** for potent inhibition of MGO-mediated AGE formation were determined using additional four flavonols (**11–14**), indicating the importance of the 3,5,7,4′-tetrahydroxy groups and the C-4 keto group in **10** (Figs. 1 and 2). The reaction of **10** with MGO in the presence of BSA and metal ions yielded four different types of products. The structures of these products were determined to be hemiacetal form of di-MGO adduct (**18**), two hemiacetal forms of mono-MGO adducts (**16** and **17**), and 3,4-dihydroxybenzoic acid (**15**), respectively (Table 1, Figs. 3–6). Under the conventional conditions, the oxidative degradation of **10** was accelerated by MGO to form 3,4-dihydroxybenzoic acid (**15**). By contrast, predominant accumulation of di-MGO adduct (**18**) was observed under oxygen-free conditions, while degradation of **18** was suppressed (Fig. 3). The C-6 and C-8 positions of the A ring in quercetin (**10**) were the major reactive sites for trapping MGO to form both mono-MGO and di-MGO adducts, and molecular oxygen oxidized di-MGO adduct (**18**) to quinone methide by generating hydrogen peroxide (Fig. 4). Inai et al. proposed a similar mechanism for oxidative degradation of quercetin (**10**) via quinone fornation, water addition, and hydrolysis.[30] However, the final step including C-C bond cleavage by hydrolysis is unlikely in view of organic chemistry. Cleavage of α-dicarbonyl compounds via Baeyer–Villiger-like rearrangement was unambiguously evidenced in our previous work,[31] thus hydrogen peroxide would attack the carbonyl group to afford acid anhydride. Hydrolysis of acid anhydride would yield 3,4-dihydroxybenzoic acid (**15**) as indicated in Fig. 4.

In this article, we proposed three different efficacies of quercetin (**10**) for inhibiting AGE formation. First, **10** functions as a metal chelating agent having catechol moiety and two other chelating sites,[32] which suppress glucose-mediated AGE formation. Excess amount of glucose in human tissues is converted into 3-deoxy glucosone (3DG) via Maillad reaction that leads to formation of such AGEs as glucosepane, versperlysine, and GLUCOLD.[17] Second, **10** traps two equivalents of MGO, one of the major causes of accumulations of AGEs in human tissues, and its scavenging effect results in inhibition of MGO-mediated AGE formation. Methylglyoxal (MGO) is produced via glycolysis, and its concentration is elevated in diabetic patients.[17] Excess amount of MGO leads to formation of such AGEs as MOLD, MOLDIC, and argpyrimidine.[17] Third, di-MGO adduct (**18**) derived from **10** rapidly consumes oxygen which accelerates formation of AGEs. Oxygen contributes to oxidative degradation of glucose with catalytic metals that leads to formation of pentosidine,[33] and oxidative degradation of lipid by oxygen produces glyoxal (GO) which leads to the formation of such advanced lipoxidation end products (ALEs) or AGEs as GODIC, GOLA, GOLD, and CML.[17,33]

Quercetin (**10**) has been recognized as one of the most important ingredients in herbal medicines or supplements, and the compound is found in a number of plants such as onion, cocoa powder, cranberries, lingonberries, kale, celery, broccoli, looseleaf lettuce, ripe tomatoes, and carrots.[34] In addition, all such pharmaceutical agents as aminoguanidine,[35] tenilsetam,[36,37] carnosine,[38] metformin,[39,40] and pyridoxamine,[41,42] developed for inhibiting AGE formation and preventing the development of diabetic complications, have serious side effects.[12] Thus, intervention using the food-borne polyphenols like **10** is likely to be an effective strategy to inhibit the formation of AGEs and prevent AGE-mediated processes linked to such age-related diseases as diabetes complication, Alzheimer's disease, and arteriosclerosis.[31,42,43]

Author contributions

S.M and M.U designed and directed the project. S.M performed experiments in Figs. 1–3 and Table 1. M.N.I.B performed experiments in Table 1 and Figs. 3–6. S.M, M.N.I.B, K.S, and M.U analyzed the data. M.N.I.B and M.U wrote the article. All authors have read and approved the final manuscript.

Disclosure statement

No potential conflict of interest was reported by the authors.

References

[1] Benavente-García O, Castillo J. Update on uses and properties of citrus flavonoids: new findings in anticancer, cardiovascular, and anti-inflammatory activity. J Agric Food Chem. 2008;56: 6185–6205.

[2] Matsuura N, Aradate T, Sasaki C, et al. Screening system for the Maillard reaction inhibitor from natural product extracts. J Health Sci. 2002;48:520–526.

[3] Matsuda H, Morikawa T, Ando S, et al. Structural requirements of flavonoids for nitric oxide production inhibitory activity and mechanism of action. Bioorg Med Chem. 2003;11:1995–2000.

[4] Wu CH, Yen G. Inhibitory effect of naturally occurring flavonoids on the formation of advanced glycation endproducts. J Agric Food Chem. 2005;53:3167–3173.

[5] Sang S, Shao X, Bai N, et al. Tea polyphenol (−)-epigallocatechin-3-gallate: a new trapping agent of reactive dicarbonyl species. Chem Res Toxicol. 2007;20:1862–1870.

[6] Shao X, Bai N, He K, et al. Apple polyphenols, phloretin and phloridzin: new trapping agents of reactive dicarbonyl species. Chem Res Toxicol. 2008;21:2042–2050.

[7] Lv L, Shao X, Chen H, et al. Genistein inhibits advanced glycation end product formation by trapping methylglyoxal. Chem Res Toxicol. 2011;24:579–586.

[8] Li D, Mitsuhashi S, Ubukata M. Protective effects of hesperidin derivatives and their stereoisomers against advanced glycation end-products formation. Pharm Biol. 2012;50:1531–1535.

[9] Li D, Shigetomi K, Mitsuhashi S, et al. Maillard reaction inhibitors produced by *Paecilomyces* sp. Biosci Biotechnol Biochem. 2013;77:2499–2501.

[10] Li XL, Zheng T, Sang S, et al. Quercetin inhibits advanced glycation end product formation by trapping methylglyoxal and glyoxal. J Agric Food Chem. 2014;62:12152–12158.

[11] Matsuura N, Aradate T, Kurosaka C, et al. 2014. Potent protein glycation inhibition of plantagoside in Plantago major seeds. BioMed Res Int. 2014;2014. ID 208539. Available from http://dx.doi.org/10.1155/2014/208539.

[12] Shao X, Chen H, Zhu Y, et al. Essential structural requirements and additive effects for flavonoids to scavenge methylglyoxal. J Agric Food Chem. 2014;62:3202–3210.

[13] Yoon SR, Shim SM. Inhibitory effect of polyphenols in *Houttuynia cordata* on advanced glycation end-products (AGEs) by trapping methylglyoxal. LWT-Food Sci Technol. 2014;61:158–163.

[14] Lo CY, Li S, Tan D, et al. Trapping reactions of reactive carbonyl species with tea polyphenols in simulated physiological conditions. Mol Nutr Food Res. 2006;50:1118–1128.

[15] Mira L, Fernadez MT, Santos M, et al. Interactions of flavonoids with iron and copper ions: a mechanism for their antioxidant activity. Free Radical Res. 2002;36:1199–1208.

[16] Zhang W, Chen C, Shi H, et al. Curcumin is a biologically active copper chelator with antitumor activity. Phytomedicine. 2016;23:1–8.

[17] Vistoli G, De Maddis D, Cipak A, et al. Advanced glycoxidation and lipoxidation end products (AGEs and ALEs): an overview of their mechanisms of formation. Free Radical Res. 2013;47:3–27.

[18] Han C, Lu Y, Wei Y, et al. D-ribose induces cellular protein glycation and impairs mouse spatial cognition. PLoS One. 2011;6:e24623.

[19] Ghosh S, Pandey NK, Roy AS, et al. Prolonged glycation of hen egg white lysozyme generates non amyloidal structures. PLoS One. 2013;8:e74336.

[20] Luckey TD, Venugopal B. Metal toxicity in mammals. Vol. 1, Physiologic and chemical basis for metal toxicity. New York (NY): Springer; 1977.

[21] Symons MCR, Benbow JA, Pelmore H. Study of calcium ion binding to D-ribose in aqueous solutions using hydroxy-proton resonance shifts. J Chem Soc Faraday Trans 1. 1982;78:3671–3677.

[22] Ye Y, Liu Q, Wang J. Influence of saccharides chelating agent on particle size and magnetic properties of Co_2 Z hexaferrite synthesized by sol–gel method. J Sol–Gel Sci Technol. 2011;60:41–47.

[23] Di Costanzo L, Flores LV, Christianson DW. Stereochemistry of guanidine-metal interactions: Implications for L-arginine-metal interactions in protein structure and function. Proteins. 2006;65: 637–642.

[24] Gold MH, Youngs HL, Sollewijn G, et al. In: Sigel A, Sigel H, editors. Metal ions in biological systems: manganese and its role in biological processes. Vol. 37, New York (NY): Marcel Dekker, Inc; 2000. p. 559–586.

[25] Shamsi FA, Partal A, Sady C, et al. Immunological evidence for methylglyoxal-derived modifications *in vivo*. Determination of antigenic epitopes. J Biol Chem. 1998;273:6928–6936.

[26] Beisswenger P, Howell S, Nelson R, et al. α-Oxoaldehyde metabolism and diabetic complications. Biochem Soc Trans. 2003;31: 1358–1363.

[27] Kilhovd BK, Juutilainen A, Lehto S, et al. Increased serum levels of methylglyoxal-derived hydroimidazolone-AGE are associated with increased cardiovascular disease mortality in nondiabetic women. Atherosclerosis. 2009;205:590–594.

[28] Thomas M, Baynes J, Thorpe S, et al. The role of AGEs and AGE inhibitors in diabetic cardiovascular disease. Curr Drug Targets. 2005;6:453–474.

[29] Cervantes-Laurean D, Schramm DD, Jacobson EL, et al. Inhibition of advanced glycation end product formation on collagen by rutin and its metabolites. J Nutr Biochem. 2006;17:531–540.

[30] Inai M, Miura Y, Honda S, et al. Metmyoglobin reduction by polyphenols and mechanism of the conversion of metmyoglobin to oxymyoglobin by quercetin. J Agric Food Chem. 2014;62: 893–901.

[31] Nagamatsu R, Mitsuhashi S, Shigetomi K, et al. Cleavage of α-dicarbonyl compounds by terpene hydroperoxide. Biosci Biotechnol Biochem. 2012;76:1904–1908.

[32] Kasprzak MM, Erxleben A, Ochocki J. Properties and applications of flavonoid metal complexes. RSC Adv. 2015;5: 45853–45877.

[33] Peyroux J, Sternberg M. Advanced glycation endproducts (AGEs): pharmacological inhibition in diabetes. Pathol Biol. 2006;54:405–419.

[34] Aguirre L, Arias N, Macarulla MT, et al. Beneficial effects of quercetin on obesity and diabetes. Open Nutraceuticals J. 2011; 4:189–198.

[35] Thomas MC, Baynes JW, Thorpe SR, et al. The role of AGEs and AGE inhibitors in diabetic cardiovascular disease. Curr Drug Targets. 2005;6:453–474.

[36] Webster J, Urban C, Berbaum K, et al. The carbonyl scavengers aminoguanidine and tenilsetam protect against the neurotoxic effects of methylglyoxal. Neurotoxic Res. 2005;7:95–101.

[37] Price DL, Rhett PM, Thorpe SR, et al. Chelating activity of advanced glycation end-product inhibitors. J Biol Chem. 2001; 276:48967–48972.

[38] Beisswenger P, Ruggiero-Lopez D. Metformin inhibition of glycation processes. Diabetes Metab. 2003;29:6S95–6S103.

[39] Beisswenger PJ, Howell SK, Touchette AD, et al. Metformin reduces systemic methylglyoxal levels in type 2 diabetes. Diabetes. 1999;48:198–202.

[40] Nagaraj RH. Effect of pyridoxamine on chemical modification of proteins by carbonyls in diabetic rats: characterization of a major product from the reaction of pyridoxamine and methylglyoxal. Arch Biochem Biophys. 2002;402:110–119.

[41] Voziyan PA, Metz TO, Baynes JW, et al. A post-amadori inhibitor pyridoxamine also inhibits chemical modification of proteins by scavenging carbonyl intermediates of carbohydrate and lipid degradation. J Biol Chem. 2002;277:3397–3403.

[42] Reddy VP, Zhu X, Perry G, et al. Oxidative stress in diabetes and Alzheimer's disease. J Alzheimers Dis. 2009;16:763–774.

[43] Jahan H, Choudhary MI. Glycation, carbonyl stress and AGEs inhibitors: a patent review. Expert Opin Ther Pat. 2015;25: 1267–1284.